Lipids (2013) 48:1237–1251
DOI 10.1007/s11745-013-3851-x

ORIGINAL ARTICLE

Identification of Plasmalogen Cardiolipins from *Pectinatus* by Liquid Chromatography–High Resolution Electrospray Ionization Tandem Mass Spectrometry

Tomáš Řezanka · Dagmar Matoulková · Lucie Kyselová · Karel Sigler

Received: 6 June 2013 / Accepted: 26 September 2013 / Published online: 10 October 2013

Abstract High resolution electrospray ionization tandem mass spectrometry (HR-ESI–MS/MS) was used to analyze cardiolipins (Ptd_2Gro) including their plasmalogen forms from three species of the anaerobic beer-spoilage bacterial genus *Pectinatus*. Cardiolipins including their plasmalogens were analyzed by HR-ESI–MS/MS on Orbitrap and almost 100 cardiolipins (i.e. tetra-acyl—Ptd_2Gro, plasmenyl-tri-acyl—$PlsPtd_2Gro$, and di-plasmenyl-di-acyl—Pls_2Ptd_2Gro) of three classes were identified. The structures of the molecular species that consist of various regioisomers and structurally similar compounds were revealed in detail. The high resolution mass spectrometry allowed the unambiguous structural assignment of Ptd_2Gro, $PlsPtd_2Gro$, and Pls_2Ptd_2Gro in the three species of *Pectinatus*, which contain predominantly odd numbered fatty acids.

Keywords *Pectinatus* · Plasmalogens · Cardiolipins · Liquid chromatography–electrospray tandem mass spectrometry

Electronic supplementary material The online version of this article (doi:10.1007/s11745-013-3851-x) contains supplementary material, which is available to authorized users.

T. Řezanka (✉) · K. Sigler
Institute of Microbiology, Academy of Sciences of the Czech Republic, Vídeňská 1083, 14220 Prague, Czech Republic
e-mail: rezanka@biomed.cas.cz

D. Matoulková
Research Institute of Brewing and Malting, Lípová 511/15, 12000 Prague, Czech Republic

L. Kyselová
Department of Biotechnology, Institute of Chemical Technology Prague, Technická 5, 16628 Prague, Czech Republic

Abbreviations

CID	Collision-induced dissociation
DSMZ	Deutsche Sammlung von Mikroorganismen und Zellkulturen
FA	Fatty acid(s)
FAME	Fatty acid methyl ester(s)
GC–MS	Gas chromatography–mass spectrometry
HILIC	Hydrophilic interaction liquid chromatography
HR-ESI–MS	High resolution electro spray mass spectrometry
LC/ESI–MS/MS	Liquid chromatography–electrospray ionization tandem mass spectrometry
PIsOH	Phosphatidylinositol
Pls_2Ptd_2Gro	Diplasmenyl-diacyl-cardiolipin
$PlsPtd_2Gro$	Plasmenyl-triacyl-cardiolipin
Ptd_2Gro	Cardiolipin
PtdEtn	Phosphatidylethanolamine
PtdGro	Phosphatidylglycerol
PtdOH	Phosphatidic acid
RIBM	Research Institute of Brewing and Malting
TLC	Thin layer chromatography

Introduction

Though beer has high microbiological stability [1], some bacteria and also wild yeasts and molds [2, 3] can still grow and multiply in wort and beer and affect beer quality. In particular, low-alcohol, nonalcoholic and nonpasteurized beers [4] are especially prone to spoilage by strict anaerobes [5] such as the strictly anaerobic bacteria of the genera *Megasphaera* and *Pectinatus*

belonging to the bacterial family Veillonellaceae [1]. Three beer-contaminating *Pectinatus* species, *Pectinatus cerevisiiphilus*, *P. frisingensis* and *P. haikarae*, were found only in brewery environments and may be associated with biofilm occurrence [3], while another species, *P. brassicae*, has recently been isolated from salty pickle wastewater [6].

Beers infected by *Pectinatus* exhibit strong haze and sediment, and an unpleasant taste and odor caused by volatile compounds, e.g. short chain acids, acetoin and hydrogen sulfide [7]. Early detection of spoilage bacteria is therefore important. Traditional detection methods involve a prolonged incubation on special diagnostic/selective media [8–10]. Alternative approaches include epifluorescence microscopy, immunofluorescence [10] or genetic methods such as PCR [11] and oligonucleotide microarrays [12].

A promising detection method is analysis of *O*-alk-1′-enyl (plasmenyl) chains of plasmalogens, derivatives of *sn*-glycero-3-phosphoric acid containing an *O*-alk-1′-enyl residue attached to the glycerol moiety in the *sn*-1 position and a polar head consisting of a nitrogenous base or glycerol moiety. They occur only in strictly anaerobic bacteria but not in aerobic or facultatively anaerobic bacteria [13].

Plasmalogen forms of phosphatidylglycerol (PtdGro) and cardiolipin (Ptd_2Gro) are the major anionic membrane lipids in most anaerobic bacteria [14]. Cardiolipins containing one or two plasmenyl chains and also those without plasmenyl were identified by Goldfine et al. [15–18] using ESI–MS/MS in bacteria of the genus *Clostridium* (*C. tetani* strain ATCC 454, *Clostridium botulinum* strains HAH, ATCC 3,502, Eklund 17B or *C. novyi* NT).

Identification of the cardiolipins is relatively difficult in bacteria which contain tens of molecular species and also mixtures of Pls_2Ptd_2Gro, $PlsPtd_2Gro$ and Ptd_2Gro found, e.g., in the genus *Clostridium* [16–19]. HPLC, especially in combination with mass spectrometry, including tandem mass spectrometry is a method of choice [20, 21].

Intact plasmalogens have been separated [22–25] from phospholipids by HPLC on diol columns [19]. The authors of [26–28] used a diol-HPLC column and a mixture of up to six solvents [27].

Identification of intact cardiolipins has been described by, e.g., Hsu et al. [29, 30] identified Ptd_2Gro by ESI–MS or ESI–MS/MS and performed its cleavage to give characteristic fragments.

This report is part of our investigation of bacterial lipids [31, 32]. It concerns the identification by LC–ESI–MS/MS of intact Ptd_2Gro, $PlsPtd_2Gro$, and Pls_2Ptd_2Gro (Fig. 1S Supplements) and their separation from diacyl phospholipids of the three *Pectinatus* species.

Materials and Methods

Standard

The standard lipids 1′,3′-bis[1,2-dimyristoyl-*sn*-glycero-3-phospho]-*sn*-glycerol (sodium salt) and 1′,3′-bis[1,2-dioleoyl-*sn*-glycero-3-phospho]-*sn*-glycerol (sodium salt) used in the experiments to verify the bacterial compound structure were purchased from Avanti Polar Lipids (Alabaster, AL, USA).

Bacterial Strains

Bacterial strains *P. cerevisiiphilus* DSM 20467^T and *P. haikarae* DSM 16980^T were purchased from the DSMZ Collection (Deutsche Sammlung von Mikroorganismen und Zellkulturen, Braunschweig, Germany). Strain *P. frisingensis* RIBM 2-86 was obtained from the RIBM Collection (Research Institute of Brewing and Malting, Prague, Czech Republic). All strains originated from a brewery environment, e.g. spoilt beer or brewery equipment.

Cultivation

Strains were grown in a modified MRS broth (medium according to de Man, Rogosa, and Sharpe, Merck, Darmstadt, Germany) supplemented with cysteine hydrochloride (0.5 g/L) and sodium thioglycollate (0.5 g/L), pH 5.6–5.7, for 72 h at 28 °C. Cultivation was performed under aerobic conditions (8 L of modified MRS broth in 10-L flasks, the surface of the medium was covered with sterile mineral oil to ensure anaerobiosis). No anaerobic atmosphere is needed if the medium is freshly prepared, is not stirred, the transfer of culture by pipette is quick and the inoculum is placed at the bottom of the test tube. After cultivation and centrifugation (10 min/6,000 rpm/4 °C), the biomass was transferred to new tubes, chilled on ice and lyophilized.

Isolation

The extraction procedure was based on the method of Bligh and Dyer [33], except that 2-propanol was substituted for methanol, since isopropanol does not serve as a substrate for phospholipases [34]. The alcohol-water mixture was cooled, one part chloroform was added and the lipids were extracted for 30 min. Insoluble material was sedimented by centrifugation and the supernatant was separated into two phases. The aqueous phase was aspirated off and the chloroform phase was washed three times with two parts 1 M KCl each [35]. The resulting chloroform phase was evaporated to dryness under reduced pressure.

First, total lipid extracts were applied to Sep-Pak Cartridge Vac 35 cc (waters; with 10 g of aminopropylsilica-based polar bonded phase), and from the cartridge were subsequently eluted nonacidic lipids with 40 mL of chloroform–methanol (70:30), and acidic lipids with 30 mL of chloroform–methanol-concentrated aqueous ammonia (69:29:2) containing 0.4 % (w/v) ammonium acetate. The eluate containing acidic lipids was reduced in volume and subjected to LC–MS.

Mild acidic hydrolysis was performed according to Johnston et al. [36]. Briefly, total lipids (0.5 mg) were hydrolyzed by a mixture of chloroform/methanol/2 M HC1 (0.4:0.4:0.4 mL). The mixture was vortex mixed and incubated at 50 °C for 3 min [36], cooled to 0 °C and neutralized by 0.7 mL 1.5 M ammonium hydroxide. The acid-stable lipids (without plasmalogens) were injected into the LC–MS apparatus.

LC–MS

The HPLC equipment consisted of a 1,090 Win system, PV5 ternary pump and automatic injector (HP 1,090 series, Hewlett Packard, USA), and two Ascentis® Express HILIC HPLC columns [5 μm particle size, L × I.D. 25 cm × 2.1 mm (Supelco, Prague)], with an injection volume of 10 μL. LC was performed at a flow rate of 0.45 mL/min for the phospholipids from all three strains, with a linear gradient from the mobile phase containing methanol/acetonitrile/aqueous 1 mM ammonium acetate (50:30:20, v/v/v) to methanol/acetonitrile/aqueous 1 mM ammonium acetate (10:70:20, v/v/v) for 60 min. The whole HPLC flow was introduced into the ESI source without any splitting.

The detector was an Applied Biosystems Sciex API 4,000 mass spectrometer (Applied Biosystems Sciex, Ontario, Canada) using electrospray mass spectra. The ionization mode was positive, the nebulizing gas (N_2) pressure was 345 kPa and the drying gas (N_2) flow and temperature were 9 L/min and 300 °C, respectively. The electrospray needle was at ground potential, whereas the capillary tension was held at 3,900 V. The cone voltage was kept at 240 V. The mass resolution was 0.1 Da and the peak width was set to 6 s. For an analysis, total ion currents (full scan) were acquired from 200 to 1,900 Da.

CID ions mass spectra were acquired by colliding the Q1 selected precursor ions with Ar gas at a collision target gas and applying collision energy of 50 eV in Q2. Scanning range of Q3 was *m/z* 200–1,900 with a step size of *m/z* 0.3 and a dwell time of 1 ms. A peak threshold of 0.3 % intensity was applied to the mass spectra. The instrument was interfaced to a computer running Applied Biosystems Analyst version 1.4.1 software.

The high resolution hybrid mass spectrometer LTQ Orbitrap Velos (Thermo Scientific, FL, USA) was used. ESI–MS analysis was performed in the negative ion mode. MS spectra were obtained with the FT mode. MS spectra were acquired with a target mass resolution of $R = 30{,}000$ at *m/z* 400 (lock mass 413.6662 Da). The ion spray voltage was set at −2,500 V and the scan range of the instruments was set at *m/z* 200–1,500. Nitrogen was used as the nebulizer gas—set at 18 arbitrary units (sheath gas) and seven arbitrary units (aux gas). Helium was used as the collision gas for CID experiments. The CID normalization energy of 35 % was used for the fragmentation of precursor ions. The MS/MS product ions were detected in the low resolution FT mode.

Results and Discussion

The yield of lyophilized cells of the three strains of genus *Pectinatus*) and the yield of lipids obtained by the Bligh–Dyer [33] extraction of lyophilized cells is shown in Table 1. Total lipids were separated on cartridges with aminopropyl silica-based rinsed in a $CHCl_3$–MeOH solvent and phospholipids were further eluted by the same solvents with concentrated aqueous ammonia.

The chromatographic conditions have been described previously [32, 37]. Figure 1 shows part of the reconstructed-ion chromatogram of total phospholipids from 21.5 to 22.5 min, i.e. in the interval in which Ptd_2Gro are eluted, see our preceding studies [32, 37]. Despite the use of a column having 25,400 theoretical plates, as determined based on a commercially obtained internal standard, i.e. sodium salt of 14:0/14:0/14:0/14:0-Ptd_2Gro, we did not succeed in separating Ptd_2Gro, $PlsPtd_2Gro$, and Pls_2Ptd_2Gro.

Cardiolipin plasmalogens are unfortunately not commercially available and the separation cannot thus be

Table 1 Yields of biomass, total lipids and phospholipids of *Pectinatus cerevisiiphilus* DSM 20467^T *P. haikarae* DSM 16980^T, and *P. frisingensis* RIBM 2-86

	DSM 20467^T	DSM 16980^T	RIBM 2-86
Biomass in g[a]	37.55	41.42	39.82
Total lipids in g	1.47	1.53	1.71
Phospholipids in mg[a]	720.3	887.4	735.3
Cardiolipins including plasmalogens[b]	10.8	16.6	12.5

[a] Data were obtained by weighing and by means of Sep-Pak Cartridge with aminopropylsilica-based polar bonded phase

[b] Data were obtained by total ion current ESI–MS (by addition of internal standard—sodium salt of 1′,3′-bis[1,2-dimyristoyl-*sn*-glycero-3-phospho]-*sn*-glycerol)

optimized by using compounds of a known structure. When using high resolution SIM (selected ion monitoring) at *m/z* 1,311.837, 1,311.873, and 1,311.910, respectively, the same figure shows the presence of all three cardiolipins. The mass tolerance was ±0.0005 Da. Unlike the base-line separation of phosphatidic acid and plasmalogen phosphatidic acid we did not succeed in separating Ptd_2Gro and $PlsPtd_2Gro$ or Pls_2Ptd_2Gro. The identities of plasmenylacyl- and acyl-cardiolipin peaks with very similar retention times in HILIC, were confirmed by high resolution ESI–MS, see Fig. 2. The successive mild acid hydrolysis of cardiolipin plasmalogens by HCl results in the formation of the corresponding lyso lipid, i.e. with the remaining *sn*-2 acyl chain and long-chain aldehydes. HCl hydrolysis of the Pls_2Ptd_2Gro results in the formation of bis-lyso-Ptd_2Gro, and hydrolysis of $PlsPtd_2Gro$ results in the formation of lyso-Ptd_2Gro in addition to long-chain aldehydes [36, 38].

Unlike the fragmentation of Ptd_2Gro, which has already been described but that of plasmalogen Ptd_2Gro has not been described. ESI tandem mass spectra of cardiolipins as monosodiated $[M\text{-}2H + Na]^-$ adduct molecular ions, arising from ubiquitous sodium salt in the sample, show loss of some different neutral moieties, chiefly acyl substituents at the *sn*-1, or *sn*-2, and *sn*-1′ or *sn*-2′ positions, exceptionally *sn*-1 (*sn*-1′) (1-*O*-alk-1′-enyl) of plasmalogen (Fig. 3).

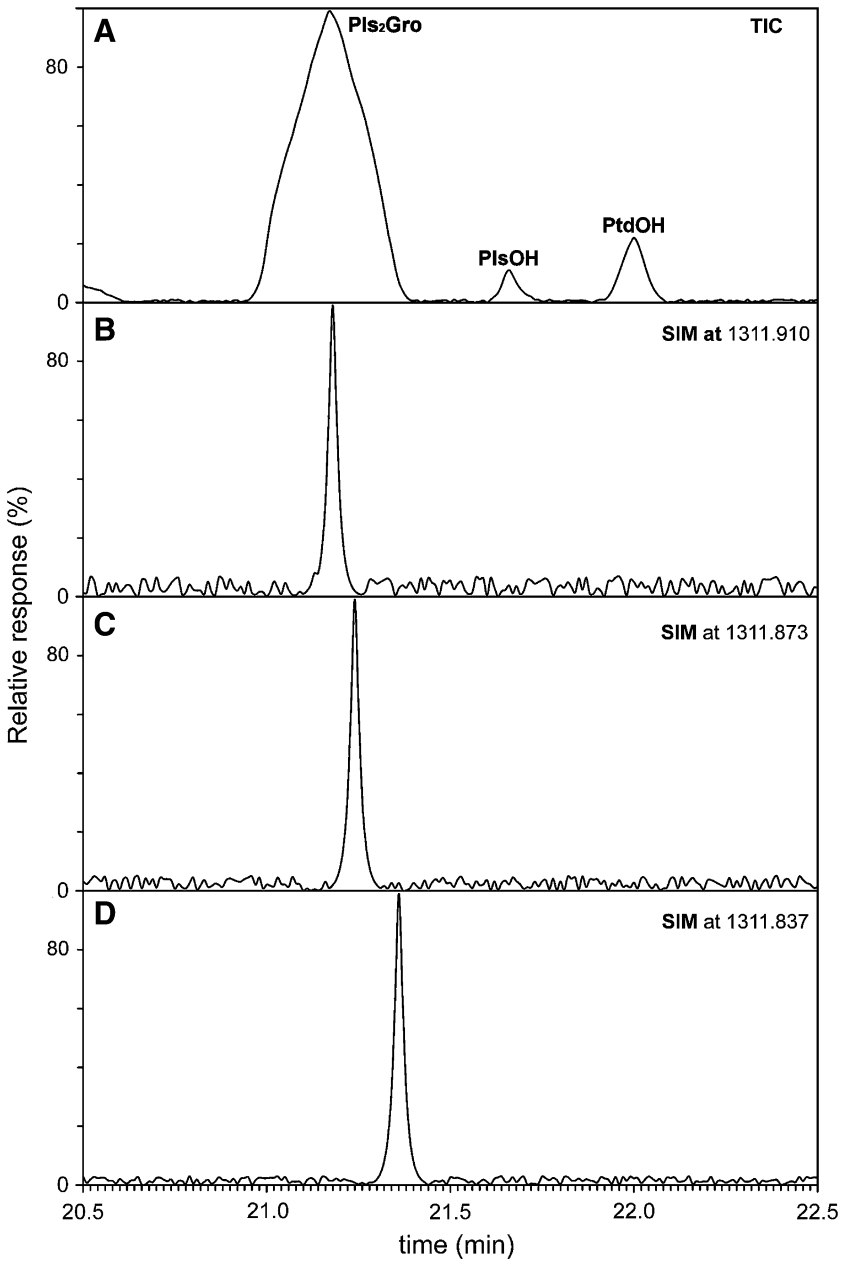

Fig. 1 Typical reconstructed-ion chromatogram of total phospholipids from *P. haikarae* and cardiolipin molecular species having 1,311 Da (**a**). The individual species correspond to *m/z* 1,311.837 (Ptd_2Gro—15:1/15:1/15:1/15:0) (**b**), 1,311.873 ($PlsPtd_2Gro$—15:1/15:1/p15:0/16:0) (**c**), and 1,311.910 (Pls_2Ptd_2Gro—p17:1/15:0/p15:0/15:0) (**d**), PlsOH is plasmalogen phosphatidic acid, PtdOH is phosphatidic acid

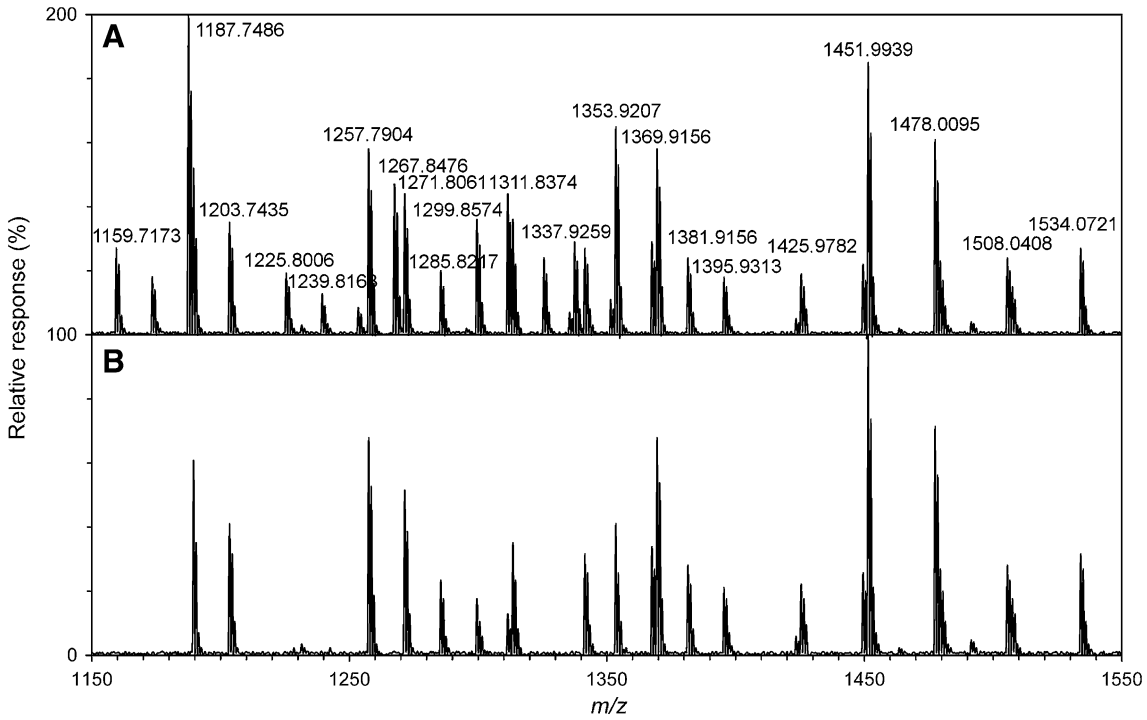

Fig. 2 High resolution electrospray mass spectrum (ESI–MS) of cardiolipins from *P. haikarae*, before (**a**) and after (**b**) acidic hydrolysis, for experimental conditions, see "Materials and Methods". *Numbers* correspond to the accurate mass values

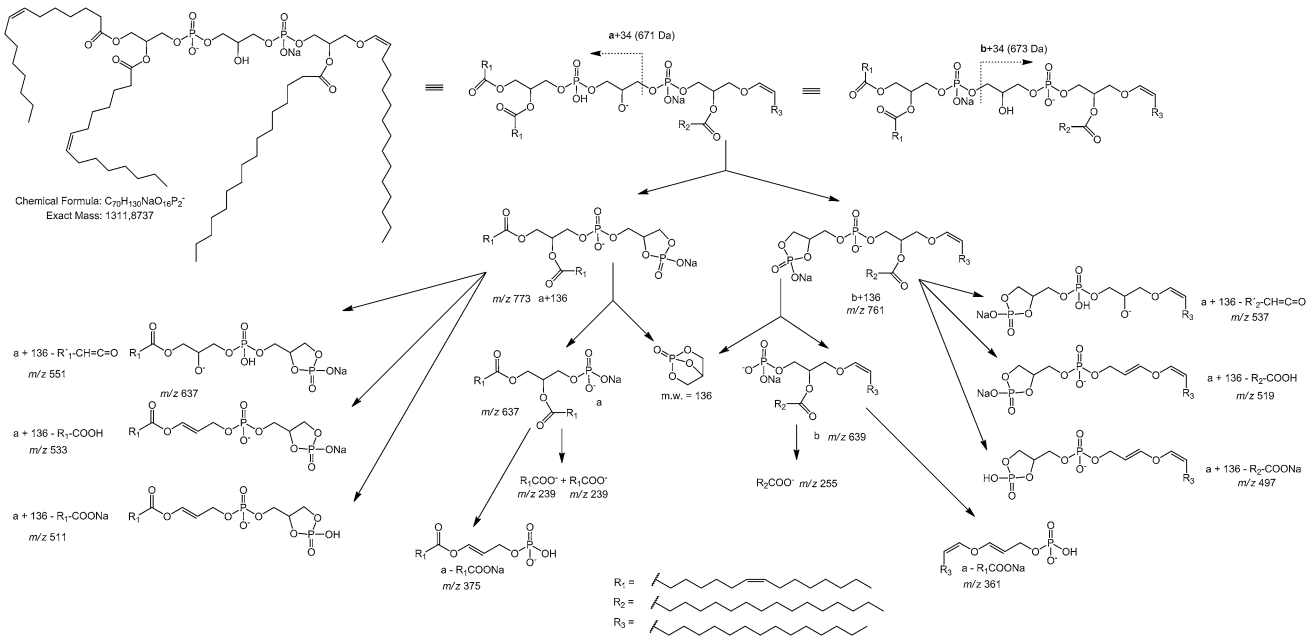

Fig. 3 The major fragmentation pathways proposed for formation of ions from the $[M\text{-}2H + Na]^-$ ion of cardiolipin ($PlsPtd_2Gro$—15:1/15:1/p15:0/15:1)

Ptd_2Gro and its plasmalogen form were abundant phospholipids. Structural characterization of Ptd_2Gro is complicated by numerous homologues that consist of various isomers (Table 2). Identification of individual molecular species was based on tandem MS.

Figure 4 shows the partial mass spectrum from Fig. 2 measured at high resolution ESI (HR-ESI–MS). The ion at *m/z* 1,311 is clearly seen to be composed of three $[M\text{-}2H + Na]^-$ ions belonging to three different molecular species, i.e. 60:3, 61:2, and 62:1 (Ptd_2Gro—15:1/15:1/15:1/

Table 2 The content of molecular species of cardiolipins including their plasmalogen forms in the three strains of *Pectinatus cerevisiiphilus* DSM 20467^T *P. haikarae* DSM 16980^T, and *P. frisingensis* RIBM 2-86

sn-1	*sn*-2	*sn*-1′	*sn*-2′	Sum C	Sum DB	[M-2H + Na]$^-$ (Da)	DSM 20467^T		DSM 16980^T		RIBM 2-86	
							R.a.[b]	I.a.[c]	R.a.[b]	I.a.[c]	R.a.[b]	I.a.[c]
17:1[a]	11:0	11:0	11:0	50	1	1,159.7172	2.4	–	2.1	–	2.7	–
11:0	11:0	18:1[a]	11:0	51	1	1,173.7328	1.6	–	1.7	–	1.4	–
11:0	11:0	17:1	11:0	50	1	1,175.7121	4.8	55	3.9	30	3.2	40
11:0	17:1	11:0	11:0	50	1	1,175.7121	–	45	–	70	–	60
11:0	11:0	19:1[a]	11:0	52	1	1,187.7485	8.7	–	10.5	–	7.6	–
11:0	11:0	18:1	11:0	51	1	1,189.7277	2.4	60	2.1	50	2.6	40
11:0	11:0	11:0	18:1	51	1	1,189.7277	–	40	–	50	–	60
11:0	11:0	19:1	11:0	52	1	1,203.7434	3.1	–	2.9	–	3.0	–
17:1[a]	11:0	17:1[a]	11:0	56	2	1,225.8005	1.7	–	1.6	–	1.5	–
11:0	14:0	18:1	11:0	54	1	1,231.7747	0.3	30	0.5	40	0.4	30
14:0	11:0	18:1	11:0	54	1	1,231.7747	–	40	–	40	–	30
18:1	11:0	14:0	11:0	54	1	1,231.7747	–	30	–	30	–	40
17:1[a]	11:0	18:1[a]	11:0	57	2	1,239.8162	1.1	–	1.2	–	1.3	–
18:1[a]	11:0	18:1[a]	11:0	58	2	1,253.8318	0.7	–	0.8	–	0.6	–
11:0	17:1	17:1	11:0	56	2	1,257.7903	4.7	55	4.1	30	3.9	50
17:1	11:0	17:1	11:0	56	2	1,257.7903	–	45	–	60	–	50
18:1[a]	11:0	19:1[a]	11:0	59	2	1,267.8475	4.1	–	4.7	–	3.9	–
11:0	17:1	18:1	11:0	57	2	1,271.8060	4.2	25	2.8	20	4.7	30
11:0	17:1	11:0	18:1	57	2	1,271.8060	–	20	–	40	–	30
18:1	11:0	17:1	11:0	57	2	1,271.8060	–	35	–	20	–	30
18:1	17:1	11:0	11:0	57	2	1,271.8060	–	25	–	20	–	10
17:1[a]	14:0	18:1[a]	11:0	60	2	1,281.8631	0.1	–	0.2	–	0.1	–
11:0	18:1	18:1	11:0	58	2	1,285.8216	1.6	10	1.4	20	4.7	30
18:1	11:0	18:1	11:0	58	2	1,285.8216	–	30	–	30	–	30
18:1	11:0	11:0	18:1	58	2	1,285.8216	–	40	–	30	–	30
18:1	18:1	11:0	11:0	58	2	1,285.8216	–	10	–	20	–	10
18:1[a]	14:0	18:1[a]	11:0	61	2	1,295.8788	0.2	50	0.2	50	0.2	50
18:1[a]	11:0	18:1[a]	14:0	61	2	1,295.8788	–	50	–	50	–	50
15:0[a]	15:1	15:1	15:0	60	2	1,297.8580	0.1	–	0.1	–	0.1	–
18:1	11:0	19:1	11:0	59	2	1,299.8373	3.1	30	3.9	40	3.3	50
18:1	19:1	11:0	11:0	59	2	1,299.8373	–	40	–	30	–	30
15:0	15:0	15:1[a]	15:0	60	1	1,299.8737	–	30	–	30	–	20
15:1	15:1	15:0	15:1	60	3	1,311.8369	2.1	–	2.7	–	3.0	–
15:1	15:1	15:0[a]	16:0	61	2	1,311.8733	1.1	–	1.0	–	0.9	–
17:1[a]	15:0	15:0[a]	15:0	62	1	1,311.9097	0.9	–	0.8	–	1.0	–
14:0	17:1	18:1	11:0	60	2	1,313.8529	0.5	15	0.4	10	0.5	20
15:0	15:1	15:1	15:0	60	2	1,313.8529	–	85	–	90	–	80
15:0	15:0	15:1	15:0	60	1	1,315.8686	1.7	–	1.6	–	1.8	–
17:1[a]	15:0	15:1	15:0	62	2	1,325.8893	2.1	45	1.9	50	2.0	55
15:0	15:1	17:1[a]	15:0	62	2	1,325.8893	–	55	–	50	–	45
17:1[a]	15:1	17:1[a]	15:0	64	3	1,335.9010	0.6	–	0.6	–	0.7	–
17:1[a]	15:0	17:1[a]	15:0	64	2	1,337.9258	2.4	–	2.0	–	2.5	–
14:0	11:0	19:1	18:1	62	2	1,341.8842	2.5	5	2.2	5	2.8	10
15:0	15:1	17:1	15:0	62	2	1,341.8842	–	50	–	45	–	50
15:0	17:1	15:1	15:0	62	2	1,341.8842	–	45	–	50	–	40
15:1	15:1	19:1[a]	15:0	64	3	1,351.9050	1.0	–	0.9	–	0.8	–

Table 2 continued

sn-1	*sn*-2	*sn*-1′	*sn*-2′	Sum C	Sum DB	[M-2H + Na]$^-$ (Da)	DSM 20467^T		DSM 16980^T		RIBM 2-86	
							R.a.[b]	I.a.[c]	R.a.[b]	I.a.[c]	R.a.[b]	I.a.[c]
17:1	11:0	17:1	18:1	63	3	1,353.8842	1.6	50	1.7	40	1.9	45
18:1	17:1	17:1	11:0	63	3	1,353.8842	–	50	–	60	–	55
15:0	15:1	19:1[a]	15:0	64	2	1,353.9206	3.8	–	3.9	–	4.1	–
15:1	15:1	19:1	15:0	64	3	1,367.8999	2.7	10	2.6	15	2.9	10
17:1	11:0	18:1	18:1	64	3	1,367.8999	–	15	–	15	–	10
18:1	17:1	18:1	11:0	64	3	1,367.8999	–	15	–	15	–	15
18:1	17:1	11:0	18:1	64	3	1,367.8999	–	15	–	15	–	15
18:1	18:1	17:1	11:0	64	3	1,367.8999	–	15	–	20	–	25
17:1	15:1	17:1	15:0	64	3	1,367.8999	–	30	–	20	–	25
15:0	15:1	19:1	15:0	64	2	1,369.9155	6.6	10	7.2	5	5.8	10
15:0	17:1	17:1	15:0	64	2	1,369.9155	–	40	–	25	–	15
18:1	18:1	18:1	11:0	65	3	1,381.9155	–	5	–	10	–	10
18:1	18:1	11:0	18:1	65	3	1,381.9155	–	5	–	10	–	10
18:1	17:1	19:1	11:0	65	3	1,381.9155	–	25	–	20	–	25
18:1	19:1	17:1	11:0	65	3	1,381.9155	–	35	–	30	–	30
18:1	18:1	19:1	11:0	66	3	1,395.9312	1.3	20	1.2	20	1.6	20
18:1	18:1	11:0	19:1	66	3	1,395.9312	–	30	–	30	–	20
18:1	19:1	18:1	11:0	66	3	1,395.9312	–	20	–	30	–	30
18:1	19:1	11:0	18:1	66	3	1,395.9312	–	30	–	20	–	30
17:1	16:1	17:1	18:1	68	4	1,421.9468	0.1	–	0.1	–	0.1	–
18:1	17:1	17:1	16:0	68	3	1,423.9625	0.5	15	0.5	10	0.6	10
17:1	17:1	17:1	17:0	68	3	1,423.9625	–	85	–	90	–	90
17:0	17:1	17:1	17:0	68	2	1,425.9781	1.5	10	1.7	10	1.6	20
15:0	17:1	19:1	17:0	68	2	1,425.9781	–	45	–	40	–	40
19:1	17:1	15:0	17:0	68	2	1,425.9781	–	45	–	50	–	40
17:0	15:0	19:1	17:0	68	1	1,427.9938	0.2	–	0.2	–	0.2	–
18:1	17:1	17:1	18:1	70	4	1,449.9781	1.9	10	1.7	15	2.1	20
17:1	17:1	17:1	19:1	70	4	1,449.9781	–	90	–	85	–	80
18:1	17:1	19:1	16:0	70	3	1,451.9938	6.8	–	7.0	5	4.9	0
18:1	19:1	17:1	16:0	70	3	1,451.9938	–		–	5	–	0
17:1	17:1	19:1	17:0	70	3	1,451.9938	–		–	5	–	5
17:0	17:1	17:1	19:1	70	3	1,451.9938	–		–	5	–	10
19:1	17:1	17:1	17:0	70	3	1,451.9938	–		–	5	–	10
15:0	17:1	19:1	19:1	70	3	1,451.9938	–		–	45	–	35
19:1	19:1	17:1	15:0	70	3	1,451.9938	–		–	30	–	40
17:0	17:1	19:1	17:0	70	2	1,454.0094	0.8	15	0.7	10	0.7	15
19:1	19:1	15:0	17:0	70	2	1,454.0094	–	85	–	90	–	85
18:1	18:1	17:1	18:1	71	4	1,463.9938	0.1	–	0.1	–	0.1	–
18:1	18:1	18:1	18:1	72	4	1,478.0094	5.4	5	5.7	10	5.1	5
18:1	17:1	19:1	18:1	72	4	1,478.0094	–	10	–	10	–	5
17:1	17:1	19:1	19:1	72	4	1,478.0094	–	25	–	20	–	10
19:1	17:1	17:1	19:1	72	4	1,478.0094	–	30	–	20	–	40
19:1	19:1	17:1	17:1	72	4	1,478.0094	–	30	–	30	–	40
19:1	17:1	19:1	17:0	72	3	1,480.0251	1.0	50	0.9	45	0.9	45
19:1	19:1	17:1	17:0	72	3	1,480.0251	–	50	–	55	–	55
17:0	19:1	19:1	17:0	72	2	1,482.0407	0.1	–	0.1	–	0.1	–
18:1	18:1	19:1	18:1	73	4	1,492.0251	0.2	50	0.2	45	0.2	45

Table 2 continued

sn-1	*sn*-2	*sn*-1′	*sn*-2′	Sum C	Sum DB	[M-2H + Na]$^-$ (Da)	DSM 20467^T		DSM 16980^T		RIBM 2-86	
							R.a.[b]	I.a.[c]	R.a.[b]	I.a.[c]	R.a.[b]	I.a.[c]
18:1	19:1	18:1	18:1	73	4	1,492.0251		50	–	55	–	55
19:1	19:1	17:1	19:1	74	4	1,506.0407	2.1	–	2.2	–	2.1	–
19:1	19:1	19:1	17:0	74	3	1,508.0564	0.6	–	0.7	–	0.8	–
19:1	19:1	19:1	19:1	76	4	1,534.0720	2.9	–	2.8	–	3.0	–

[a] Plasmalogens

[b] *R.a.* relative abundance (%)—determined by HR-ESI–MS

[c] *I.a.* isomer amount (%)—determined by tandem MS by means of abundance of ions **a** and **b**, for the structures see Fig. 3

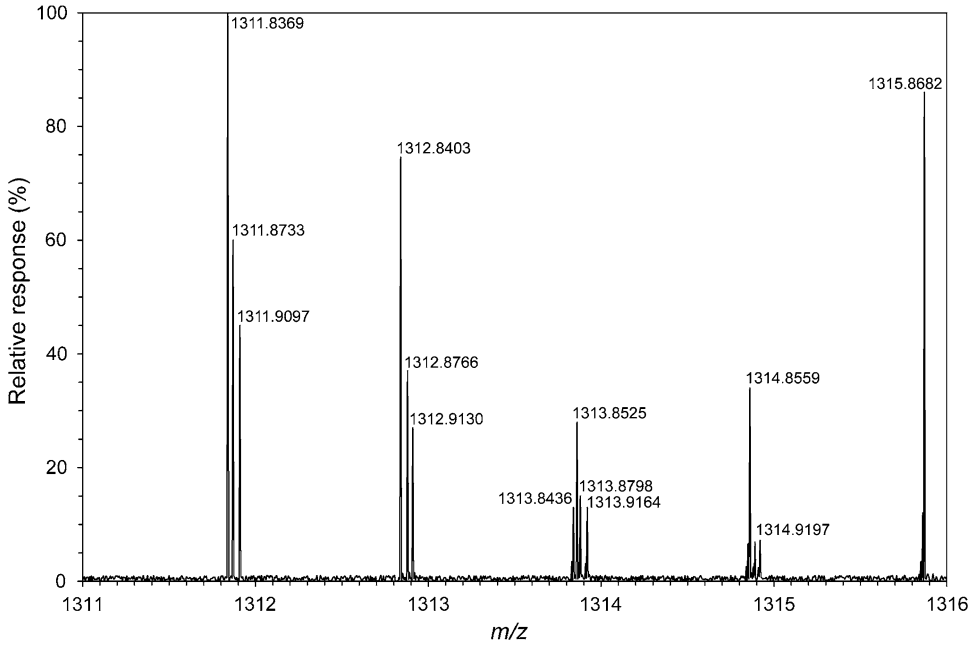

Fig. 4 A detail of the total ion current of cardiolipins (Ptd_2Gro, $PlsPtd_2Gro$, and Pls_2Ptd_2Gro) in the range of *m/z* 1,311–1,316 measured by HR-ESI–MS. For the full spectrum and conditions see Fig. 2 and "Materials and Methods"

Table 3 Nine cardiolipins with mass 1,313 Da and having combinations of 60:3, 61:2, and 62:1 (sum of acyl chains: sum of double bonds) and containing isotopes of deuterium (^2H) and ^{13}C which were identified by HR-MS–ESI

Compound	Formula (2 × ^{13}C)	*m/z*	Formula (^{13}C + D)	*m/z*	Formula (2 × D)	*m/z*
Ptd_2Gro 15:1/15:1/15:1/15:0	$^{13}C_2C_{67}H_{126}NaO_{17}P_2^-$	1,313.8435	$^{13}CC_{68}DH_{125}NaO_{17}P_2^-$	1,313.8410	$C_{69}D_2H_{124}NaO_{17}P_2^-$	1,313.8464
$PlsPtd_2Gro$ 15:1/15:1/p15:0/16:0	$^{13}C_2C_{68}H_{130}NaO_{16}P_2^-$	1,313.8799	$^{13}CC_{69}DH_{129}NaO_{16}P_2^-$	1,313.8774	$C_{69}D_2H_{128}NaO_{16}P_2^-$	1,313.8828
Pls_2Ptd_2Gro p17:1/15:0/p15:0/15:0	$^{13}C_2C_{69}H_{134}NaO_{15}P_2^-$	1,313.9163	$^{13}CC_{69}DH_{133}NaO_{15}P_2^-$	1,313.9138	$C_{69}D_2H_{132}NaO_{15}P_2^-$	1,313.9192

15:0, $PlsPtd_2Gro$—15:1/15:1/p15:0/16:0, and Pls_2Ptd_2Gro—p17:1/15:0/p15:0/15:0). The situation with the ion at *m/z* 1,313 is more complicated. This ion is, in principle, composed of 11 molecular species, two of which belong to these cardiolipins (14:0/17:1/11:0/18:1 and 15:0/15:1/15:0/15:1) and nine other cardiolipins are combinations of the above 60:3, 61:2, and 62:1 containing isotopes of deuterium (D) and ^{13}C, see Table 3. The use of HR MS thus in fact made it possible to further separate Ptd_2Gro from $PlsPtd_2Gro$ and of Pls_2Ptd_2Gro by means of MS^2.

The MS^2 spectrum of the ions at *m/z* 1,311.8 features ions at *m/z* 1,089, 1,071, and 1,049 (Fig. 5a), which arise from neutral losses of the 15:1-fatty acyl substituent as a ketene, a free acid, and as a sodium salt, respectively, while the ions at *m/z* 1,087, 1,069, and 1,047 arise from the corresponding losses of the 15:0-fatty acyl substituent.

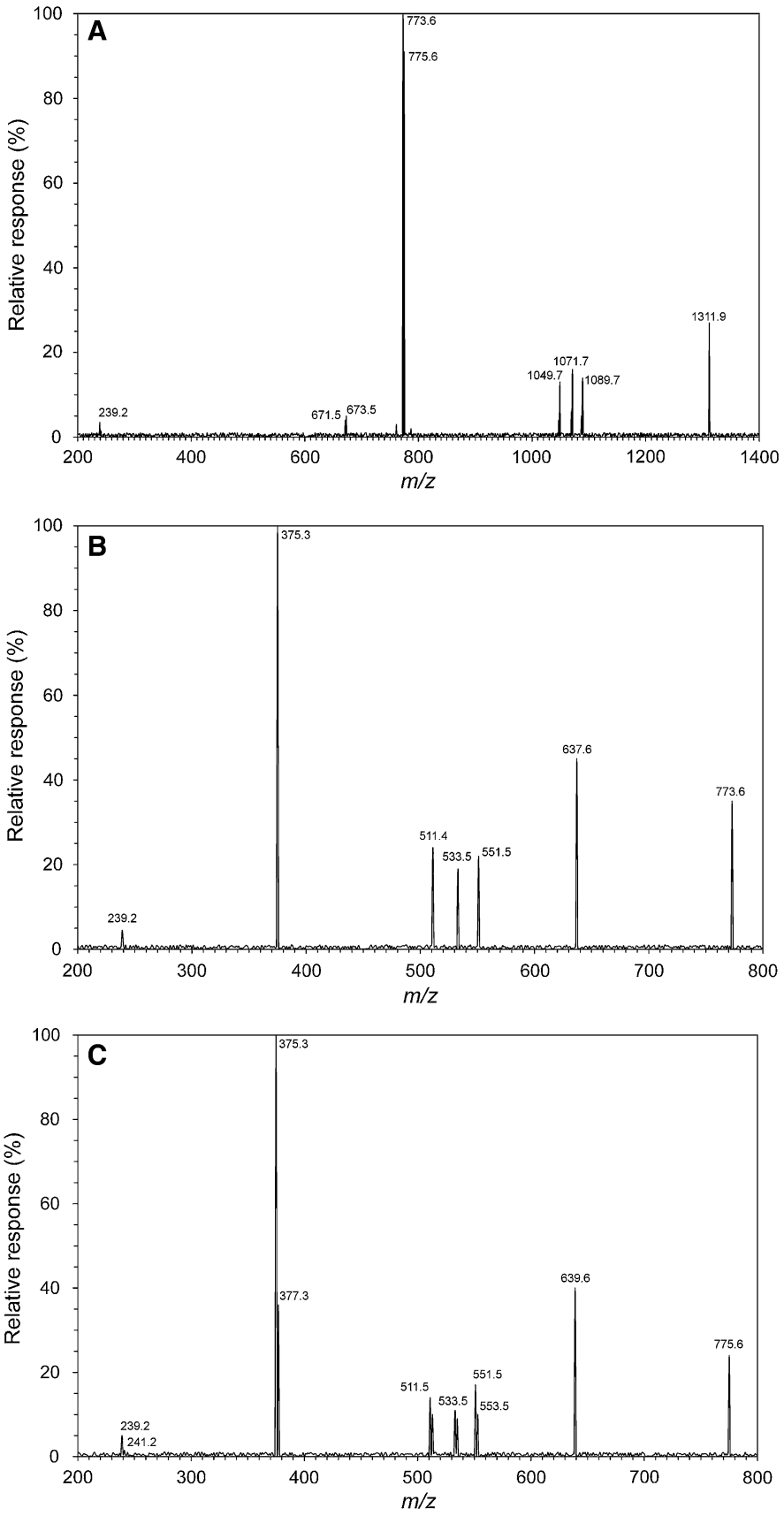

Fig. 5 The Orbitrap low resolution MS^2 and MS^3 spectra of Ptd_2Gro—15:1/15:1/15:1/15:0. **a** MS^2 spectrum of the $[M\text{-}2H + Na]^-$ ion at *m/z* 1,311.8369; **b** MS^3 spectrum of the $[\mathbf{a} + 136]^-$ ion at *m/z* 773.6 (15:1/15:1); **c** MS^3 spectrum of the $[\mathbf{b} + 136]^-$ ion at *m/z* 775.6 (15:1/15:0)

The fragmentation pathways of the $[M\text{-}2H + Na]^-$ ion of $PlsPtd_2Gro$ under CAD (MS^2) in ion-trap—Orbitrap give fragmentation that yields two prominent $[\mathbf{a} + 136]^-$ and $[\mathbf{b} + 136]^-$ ions via cleavages of the bonds, see Fig. 3. As shown in Fig. 5a, the MS^2 spectrum of the $[M\text{-}2H + Na]^-$ ion at *m/z* 1,311.8 from *P. haikarae* is dominated by the ions at *m/z* 773 and *m/z* 775, respectively, representing $[\mathbf{a} + 136]^-$ and $[\mathbf{b} + 136]^-$ ions. These ions yield ions at *m/z* 637 and *m/z* 639 (**a** and **b** ion) by loss of a bicyclic glycerophosphate ester (136 Da) [39]. The MS^2 spectrum of the *m/z* 1,311.8 ion also contains ions at *m/z* 671 $[\mathbf{a} + 34]^-$ and at *m/z* 673 $[\mathbf{b} + 34]^-$ ions, respectively, via loss of a glycerophosphatidic acid as the sodium salt (Fig. 5a).

The fragmentation pathway is also corroborated by the two MS^3 spectra, i.e. (1,311 → 773 and 1,311 → 775) (Fig. 5b and c), yielding ions at *m/z* 637 and 639, respectively. The MS^3 spectrum of the *m/z* 773 ion (1,311 → 773) (Fig. 5b) contains a major ion at *m/z* 511 (773–262) via loss of the 15:1 fatty acyl substituent as sodium salt, and ions at *m/z* 551 and 533, arising from losses of the 15:1-fatty acyl substituent as a ketene and free acid, respectively. The most abundant is the ion at *m/z* 375 arising from the ion at *m/z* 733 (773-136-$C_{14}H_{27}COONa$), i.e. sodium salt of pentadecenoic acid. This suggests that the *m/z* 773 ion represents a 15:1/15:1-structure.

The *m/z* 375 ion (775-136-$C_{14}H_{29}COONa$, i.e. 264 Da) arising from further loss of the 15:0-fatty acyl substituent

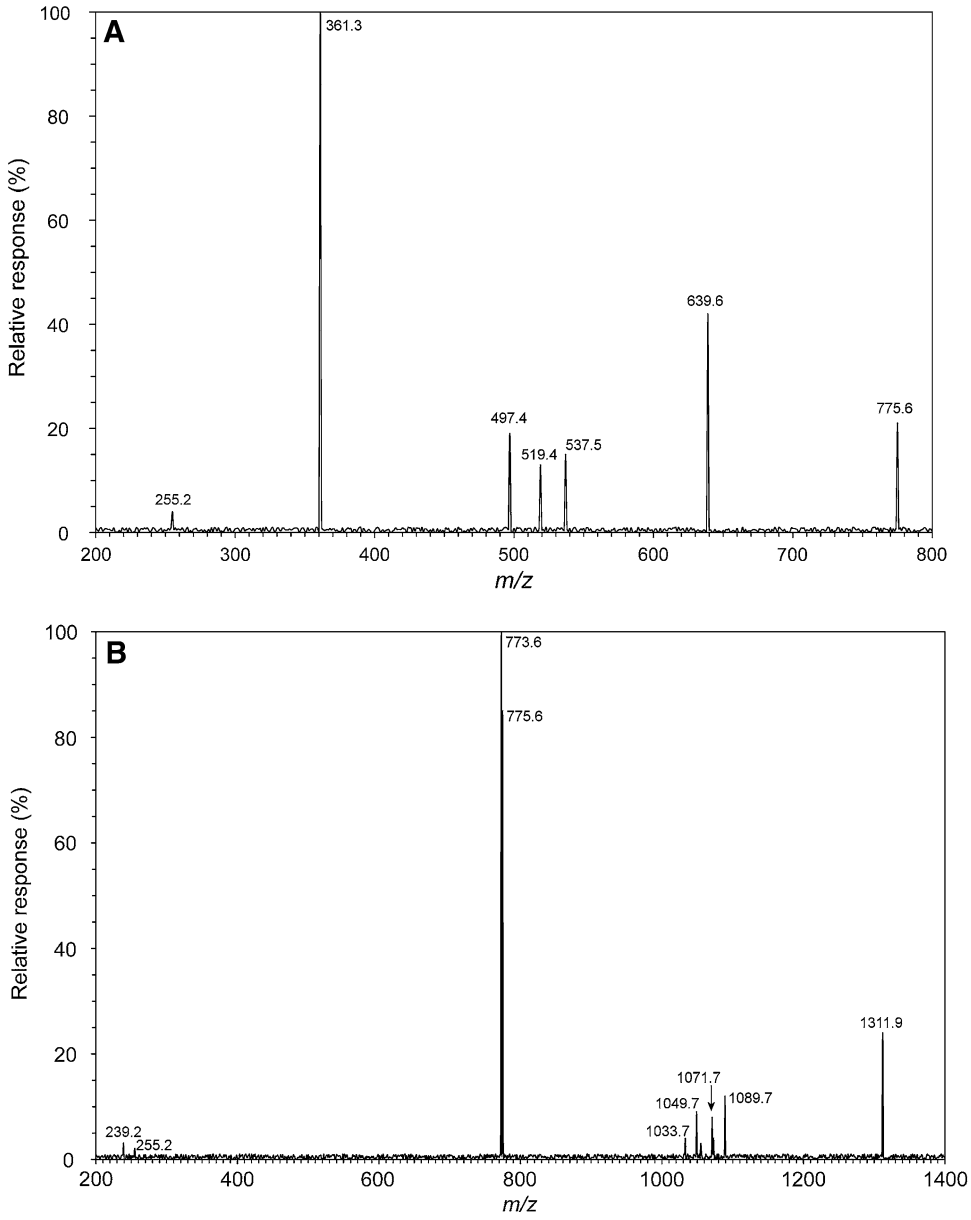

Fig. 6 The Orbitrap low resolution MS^2 and MS^3 spectra of $PlsPtd_2Gro$—15:1/15:1/p15:0/16:0. **a** MS^2 spectrum of the $[M\text{-}2H + Na]^-$ ion at *m/z* 1,311.8733; **b** MS^3-spectrum of the $[\mathbf{b} + 136]^-$ ion at *m/z* 775.6 (16:0/p15:0)

as a sodium salt is more abundant than the *m/z* 377 ion (775-136-$C_{14}H_{27}COONa$, i.e. 262 Da) arising from the analogous loss of the 15:1-fatty acyl substituent in the MS^3 spectrum of the *m/z* 775 ion (Fig. 5c). This indicates that the 15:1 and 15:0 fatty acyl moieties reside at *sn*-1′ and *sn*-2′ of the third glycerol, respectively. This was confirmed by the low-abundance ions at *m/z* 239 and *m/z* 241, i.e. $C_{14}H_{27}COO^-$ and $C_{14}H_{29}COO^-$, respectively. This assignment is also supported by the observation of a higher abundance of the *m/z* 551 ion (775–224) arising from loss of the 15:0 fatty acyl moiety at *sn*-2′ as ketene than the *m/z* 553 ion (775–222), arising from the analogous loss of the 15:1 as ketene at *sn*-1′. The above results thus demonstrate that the *m/z* 1,311.8 ion consists of a (15:1/15:1) (15:1/15:0)-Ptd_2Gro structure.

In MS^2 and MS^3 spectra, the triacyl-mono-plasmalogen 15:1/15:1/p15:0/16:0-Ptd_2Gro ($PlsPtd_2Gro$) at *m/z* 1,311.8733 exhibits a very similar fragmentation as Ptd_2Gro. The MS^2 spectrum shown in Figs. 3 and 6a indicates that fragmentation of $PlsPtd_2Gro$ yields ions similar to those arising in the fragmentation of Ptd_2Gro, see Table 4.

The MS^3 spectrum of the ion at *m/z* 773 is identical with the MS^3 spectrum of Ptd_2Gro (the spectrum is not shown), for the data see Table 5. This implies that the substituents on glycerol 1 are also identical. The MS^3 spectrum of part **b**, i.e. part of glycerol 3—the glycerol with the bound vinyl ether—is given in Fig. 6b and the relevant data are given in Table 5. The major ion is again that with the structure **b**−R_2COONa at *m/z* 361; for other ions see Fig. 6b and Table 5.

The MS^2 spectrum of Pls_2Ptd_2Gro at *m/z* 1,311.9097 is given in Fig. 7a and the data are shown in Table 4. The major ions in the MS^3 spectrum are again ions of the type of **b**−R_2COONa at *m/z* 387 and **a** + R_2COONa at *m/z* 361, respectively. The data are given in Table 5 and mass spectra are shown in Fig. 7b and c.

The content of FA was determined by GC–MS in the three species of *Pectinatus* as previously described [32]. The most abundant fatty acid was 15:0, which is fully in keeping with the most abundant molecular species of cardiolipins, i.e. *P. frisingensis* RIBM 2-86 15:0-15:1-15:0-19:1 amounting to 7.2 % total cardiolipins (Table 1S, Supplements). The most abundant aldehyde was p19:1, again in agreement with the most abundant plasmalogens, i.e. 11:0-11:0-11:0-p19:1 forming 8.7 % total cardiolipins from *P. haikarae* DSM 16,980.

By using purchased standards of two Ptd_2Gro, i.e. 1′,3′-bis[1,2-dioleoyl-*sn*-glycero-3-phospho]-*sn*-glycerol (sodium salt) and the corresponding homolog 1′,3′-bis[1,2-dimyristoyl-*sn*-glycero-3-phospho]-*sn*-glycerol (sodium salt) we found that the abundant ions at *m/z* 749 (dimyristoyl) and 857 (dioleoyl) ([**a** + 136]$^-$) and at *m/z* 613 and 721 ([**a**]$^-$) show a linear response in an interval from 1.7×10^{-7} to 8.0×10^{-4} mol/mL. For quantification of plasmalogens we assumed that they have a similar mechanism of ionization.

Table 4 Cardiolipin species at *m/z* 1,311.8373 (Ptd_2Gro—15:1/15:1/15:1/15:0), 1,311.8737 ($PlsPtd_2Gro$—15:1/15:1/p15:0/16:0), and 1,311.9101 (Pls_2Ptd_2Gro—p17:1/15:0/p15:0/15:0) identified in *P. haikarae* by MS^2

Structure of ion[a]	Ptd_2Gro		$PlsPtd_2Gro$		Pls_2Ptd_2Gro	
	m/z	%	*m/z*	%	*m/z*	%
$[R_1COO]^-$	239	3.5	239	3.1	241	4
$[R_2COO]^-$	241	1.5	255	2.1	–	–
[**a**]$^-$	637	0.9	-[b]	–	–	–
[**b**]$^-$	639	0.6	–	–	–	–
[**a** + 34]$^-$	671	4	–	–	–	–
[**b** + 34]$^-$	673	5	–	–	–	–
[**b** + 136−14]$^-$	761	3	–	–	–	–
[**a** + 136]$^-$	773	100	773	100	787	98.9
[**b** + 136]$^-$	775	91	775	85	761	100
[**a** + 136 + 14]$^-$	787	2	–	–	–	–
[M-2H + Na-RCOONa]$^-$	1,047[c]	4	1,033[e]	4	1,047[c]	11
[M-2H + Na-RCOONa]$^-$	1,049[d]	13	1,049[d]	9	–	–
[M-2H + Na-RCOOH]$^-$	1,069[c]	6	1,055[e]	3	1,069[c]	4
[M-2H + Na-RCOOH]$^-$	1,071[d]	16	1,071[d]	8	–	–
[M-2H + Na-R′CH = C = O]$^-$	1,087[c]	5	1,073[e]	4	1,087[c]	13
[M-2H + Na-R′CH = C = O]$^-$	1,089[d]	14	1,089[d]	12	–	–
[M-2H + Na]$^-$	1,311	27	1,311	24	1,311	19

[a] See Fig. 3

[b] Not detected

[c] 15:0, i.e. [M-2H + Na-RCOONa]$^-$ = [M-2H + Na-15:0 as Na salt]$^-$, etc

[d] 15:1

[e] 16:0

Identification of molecular species of phospholipids, especially of plasmalogens in bacteria has been performed very rarely [13]. Only Hsu and Turk [39] reported identification and quantification of Ptd_2Gro, but not of plasmalogen Ptd_2Gro which are absent in *Escherichia coli* as an aerobic bacterium. HR-ESI–MS was used to identify tens of molecular species, and isobaric molecular species were quantified by tandem MS.

Both Ptd_2Gro and $PlsPtd_2Gro$, as well as Pls_2Ptd_2Gro were identified in *C. botulinum*. The quantification of spots on TLC plates showed that plasmalogens are more abundant than tetra-acyl Ptd_2Gro in eight out of 12 strains [17]. ESI–MS was used to determine of tetra-acyl Ptd_2Gro as

Table 5 Cardiolipin species, i.e. Ptd_2Gro—15:1/15:1/15:1/15:0, $PlsPtd_2Gro$—15:1/15:1/p15:0/16:0, and Pls_2Ptd_2Gro—p17:1/15:0/p15:0/15:0) identified in *P. haikarae* by MS^3

Structure of ion[a]	Ptd_2Gro		$PlsPtd_2Gro$		Pls_2Ptd_2Gro	
	a = 15:1/15:1		**a** = 15:1/15:1		**a** = p17:1/15:0	
	m/z	%	*m/z*		*m/z*	%
$[\mathbf{a} + 136]^-$	773	35	773	24	787	22
$[\mathbf{a}]^-$	637	45	637	40	651	36
$[\mathbf{a} + 136\text{-}R_2'CH = C = O]^-$	551	22	551	12	563	9
$[\mathbf{a} + 136\text{-}R_1'CH = C = O]^-$	551	-[b]	551	–	–	–
$[\mathbf{a} + 136\text{-}R_2COO]^-$	533	19	533	11	545	12
$[\mathbf{a} + 136\text{-}R_1COO]^-$	533	–	533	–	–	–
$[\mathbf{a} + 136\text{-}R_2COONa]^-$	511	24	511	14	523	11
$[\mathbf{a} + 136\text{-}R_1COONa]^-$	511	–	511	–	–	–
$[\mathbf{a}\text{-}R_2COONa]^-$	375	100	375	100	387	100
$[\mathbf{a}\text{-}R_1COONa]^-$	375	–	375	–	–	–
$[R_2COO]^-$	239	4	239	5	241	4
$[R_1COO]^-$	239	–	239	–	–	–
Structure of ion[a]	Ptd_2Gro		$PlsPtd_2Gro$		Pls_2Ptd_2Gro	
	b = 15:1/15:0		**b** = 16:0/p15:0		**b** = p15:0/15:0	
	m/z	%	*m/z*	%	*m/z*	%
$[\mathbf{b} + 136]^-$	775	24	775	21	761	23
$[\mathbf{b}]^-$	639	40	639	42	625	37
$[\mathbf{b} + 136\text{-}R_1'CH = C = O]^-$	553	10	–	–	–	–
$[\mathbf{b} + 136\text{-}R_2'CH = C = O]^-$	551	17	537	15	537	7
$[\mathbf{b} + 136\text{-}R_1COO]^-$	535	11	–	–	–	–
$[\mathbf{b} + 136\text{-}R_2COO]^-$	533	9	519	13	519	9
$[\mathbf{b} + 136\text{-}R_1COONa]^-$	513	14	–	–	–	–
$[\mathbf{b} + 136\text{-}R_2COONa]^-$	511	10	497	19	497	10
$[\mathbf{b}\text{-}R_1COONa]^-$	377	100	–	–	–	–
$[\mathbf{b}\text{-}R_2COONa]^-$	375	36	361	100	361	100
$[R_1COO]^-$	241	1.5	–	–	–	–
$[R_2COO]^-$	239	5	255	4	241	5

The structures of ions derived from $[\mathbf{a} + 136]^-$ or $[\mathbf{b} + 136]^-$ ions are shown

[a] See Fig. 3

[b] Not detected

well as corresponding plasmalogens, which have a molecular weight 16 Da lower than tetra-acyl Ptd_2Gro. In cardiolipins from strain ATCC 454 Ptd_2Gro containing two plasmenyl chains were also identified. A total of ten molecular species of both Ptd_2Gro and $PlsPtd_2Gro$ from 56:0 to 64:1 were identified, with a prevalence of unsaturated Ptd_2Gro (monoenoic and dienoic), and six Pls_2Ptd_2Gro. Individual acyls or plasmenyl chains were not identified and quantification of non-plasmenyl and plasmenyl Ptd_2Gro was not performed.

The authors did not quantitatively determine plasmalogens in Ptd_2Gro but only an overall content of plasmalogens in PtdGro and Ptd_2Gro. In cardiolipin they identified Ptd_2Gro, $PlsPtd_2Gro$ and Pls_2Ptd_2Gro from 52:0 to 60:0 but again without quantification of individual molecular species [18].

Based on a previous study [39] we endeavored here to quantify individual molecular species of Ptd_2Gro, $PlsPtd_2Gro$, and Pls_2Ptd_2Gro, see Table 2. As in our previous report [32], in which we identified and quantified PtdGro and PlsGro, also here individual *Pectinatus* strains did not exhibit significant differences between cardiolipins. This is consistent with their presumed biosynthesis in which two molecules of PtdGro give rise to Ptd_2Gro [18].

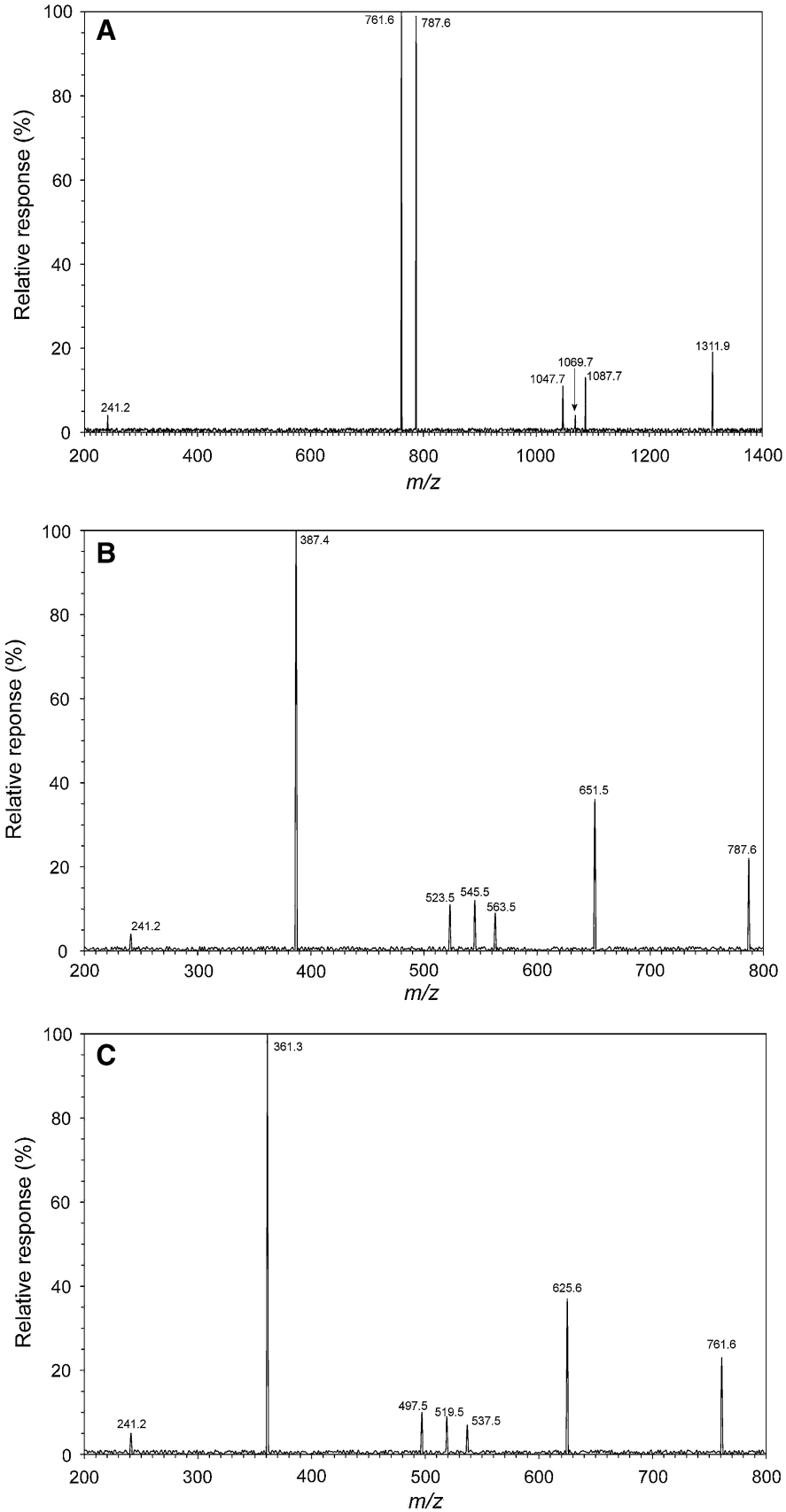

Fig. 7 The Orbitrap low resolution MS^2 and MS^3 spectra of Pls_2Ptd_2Gro—p17:1/15:0/p15:0/15:0. **a** MS^2 spectrum of the $[M\text{-}2H + Na]^-$ ion at *m/z* 1,311.9097; **b** MS^3-spectrum of the $[\mathbf{a} + 136]^-$ ion [(p17:1/15:0) at *m/z* 787.6; **c** MS^3-spectrum of the $[\mathbf{b} + 136]^-$ ion at *m/z* 761.6 (15:0/p15:0]

Conclusion

To our knowledge, detailed identification and quantitation of molecular species of plasmalogen Ptd_2Gro in bacteria is lacking. Cardiolipins were identified in the bacteria *E. coli* [39] or *Corynebacterium* [40] by means of mass spectrometry; these bacteria (included in the phylum Proteobacteria and Actinobacteria, resp.) are taxonomically relatively distant from *Pectinatus* which belongs to the phylum Firmicutes and also in *Clostridium*, which also belongs to anaerobes and is taxonomically classed to the same phylum [41].

We showed that tandem MS with HR-ESI–MS can be used for structural characterization of Ptd_2Gro [39, 42, 43] and also for plasmalogen forms. Interestingly, virtually nothing is known about the *in-vivo* physiological relevance of this Ptd_2Gro in bacterial membranes although it is assumed to function in the regulation of membrane lipid composition under anaerobiosis and in an appropriate packaging of a stable lipid bilayer. From a previous paper describing of Ptd_2Gro species [39], it is conceivable that Ptd_2Gro, $PlsPtd_2Gro$, and Pls_2Ptd_2Gro of three strains of *Pectinatus* contain predominantly odd numbered fatty acids. The distribution of these FA is different from known derivatives of Ptd_2Gro since most of fatty acids are saturated or have a cyclopropane ring. Our study emphasizes the need for including similar analyses in future taxonomic work on this and other groups [44].

Acknowledgments The research was supported by GACR P503/11/0215 and P503/12/1424, and by the Institutional Internal Project RVO 61388971.

References

1. Vaughan A, O'Sullivan T, van Sinderen D (2005) Enhancing the microbiological stability of malt and beer—a review. J Inst Brew 111(4):355–371
2. Marchandin H, Teyssier C, Campos J, Jean-Pierre H, Roger F, Gay B, Carlier JP, Jumas-Bilak E (2010) *Negativicoccus succinicivorans* gen. nov., sp. nov., isolated from human clinical samples, emended description of the family *Veillonellaceae* and description of *Negativicutes* classis nov., *Selenomonadales* ord. nov. and *Acidaminococcaceae* fam. nov. in the bacterial phylum *Firmicutes*. Int J Syst Evol Microbiol 60(6):1271–1279
3. Matoulkova D, Kosar K, Slaby M, Sigler K (2012) Occurrence and species distribution of strictly anaerobic bacterium *Pectinatus* in brewery bottling halls. J Amer Soc Brew Chem 70(4):262–267
4. Chelack BJ, Ingledew WM (1987) Anaerobic gram-negative bacteria in brewing—a review. J Amer Soc Brew Chem 45(4):123–127
5. Sakamoto K, Konings WN (2003) Beer spoilage bacteria and hop resistance. Int J Food Microbiol 89(2–3):105–124
6. Zhang WW, Fang MX, Tan HQ, Zhang XQ, Wu M, Zhu XF (2012) *Pectinatus brassicae* sp. nov., a gram-negative, anaerobic bacterium isolated from salty wastewater. Int J Syst Evol Microbiol 62(9):2145–2149
7. Jespersen L, Jakobsen M (1996) Specific spoilage organisms in breweries and laboratory media for their detection. Int J Food Microbiol 33(1):139–155
8. Matoulkova D, Kosar K, Sigler K (2012) Rapid, simple and specific cultivation-based method for detection of *Pectinatus* sp. in brewery samples. J Amer Soc Brew Chem 70(1):29–34
9. Satokari R, Juvonen R, Mallison K, von Wright A, Haikara A (1998) Detection of beer spoilage bacteria *Megasphaera* and *Pectinatus* by polymerase chain reaction and colorimetric microplate hybridization. Int J Food Microbiol 45(2):119–127
10. Juvonen R, Koivula T, Haikara A (2008) Group-specific PCR-RFLP and real-time PCR methods for detection and tentative discrimination of strictly anaerobic beer-spoilage bacteria of the class *Clostridia*. Int J Food Microbiol 125(2):162–169
11. Suzuki K (2011) 125th anniversary review: microbiological instability of beer caused by spoilage bacteria. J Inst Brew 117(2):131–155
12. Weber DG, Sahm K, Polen T, Wendisch VF, Antranikian G (2008) Oligonucleotide microarrays for the detection and identification of viable beer spoilage bacteria. J Appl Microbiol 105(4):951–962
13. Goldfine H (2010) The appearance, disappearance and reappearance of plasmalogens in evolution. Prog Lipid Res 49(4):493–498
14. Rezanka T, Kresinova Z, Kolouchova I, Sigler K (2012) Lipidomic analysis of bacterial plasmalogens. Folia Microbiol 57(5):463–472
15. Geiger O, Gonzalez-Silva N, Lopez-Lara IM, Sohlenkamp C (2010) Amino acid-containing membrane lipids in bacteria. Prog Lipid Res 49(1):46–60
16. Johnston NC, Aygun-Sunar S, Guan Z, Ribeiro AA, Daldal F, Raetz CRH, Goldfine H (2010) A phosphoethanolamine-modified glycosyl diradylglycerol in the polar lipids of *Clostridium tetani*. J Lipid Res 51(7):1953–1961
17. Guan Z, Johnston NC, Raetz CRH, Johnson EA, Goldfine H (2012) Lipid diversity among botulinum neurotoxin producing clostridia. Microbiology (United Kingdom) 158(10):2577–2584
18. Guan Z, Johnston NC, Aygun-Sunar S, Daldal F, Raetz CRH, Goldfine H (2011) Structural characterization of the polar lipids of *Clostridium novyi* NT. Further evidence for a novel anaerobic biosynthetic pathway to plasmalogens. Biochim Biophys Acta—Mol Cell Biol Lipids 1811(3):186–193
19. Christie WW, Han X (2010) Lipid analysis, 4th edn. The Oily Press, Bridgwater
20. Vaidyanathan S, Kell DB, Goodacre R (2002) Flow-injection electrospray ionization mass spectrometry of crude cell extracts for high-throughput bacterial identification. J Am Soc Mass Spectrom 13(2):118–128
21. Zhang JI, Talaty N, Costa AB, Xia Y, Tao WA, Bell R, Callahan JH, Cooks RG (2011) Rapid direct lipid profiling of bacteria using desorption electrospray ionization mass spectrometry. Int J Mass Spectr 301(1–3):37–44
22. Schwalbe-Herrmann M, Willmann J, Leibfritz D (2010) Separation of phospholipid classes by hydrophilic interaction chromatography detected by electrospray ionization mass spectrometry. J Chromatogr A 1217(32):5179–5183
23. Kamleh A, Barrett MP, Wildridge D, Burchmore RJS, Scheltema RA, Watson DG (2008) Metabolomic profiling using orbitrap Fourier transform mass spectrometry with hydrophilic interaction chromatography: a method with wide applicability to analysis of biomolecules. Rapid Commun Mass Spectrom 22(12):912–1918
24. Scherer M, Schmitz G, Liebisch G (2010) Simultaneous quantification of cardiolipin, bis(monoacylglycero)phosphate and their

precursors by hydrophilic interaction LC–MS/MS including correction of isotopic overlap. Anal Chem 82(21):8794–8799
25. Nguyen HP, Schug KA (2008) The advantages of ESI–MS detection in conjunction with HILIC mode separations: fundamentals and applications. J Sep Sci 31(9):1465–1480
26. Uran S, Larsen A, Jacobsen PB, Skotland T (2001) Analysis of phospholipid species in human blood using normal-phase liquid chromatography coupled with electrospray ionization ion-trap tandem mass spectrometry. J Chromatogr B 758(2):265–275
27. Olsson NU, Harding AJ, Harper C, Salem N (1996) High-performance liquid chromatography method with light-scattering detection for measurements of lipid class composition: analysis of brains from alcoholics. J Chromatogr B 681(2):213–218
28. Mawatari S, Okuma Y, Fujino T (2007) Separation of intact plasmalogens and all other phospholipids by a single run of high-performance liquid chromatography. Anal Biochem 370(1):54–59
29. Hsu FF, Turk J, Thukkani AK, Messner MC, Wildsmith KR, Ford DA (2003) Characterization of alkylacyl, alk-1-enylacyl and lyso subclasses of glycerophosphocholine by tandem quadrupole mass spectrometry with electrospray ionization. J Mass Spectrom 38(7):752–763
30. Hsu FF, Turk J (2005) Electrospray ionization with low-energy collisionally activated dissociation tandem mass spectrometry of complex lipids: structural characterization and mechanisms of fragmentation. In: Byrdwell WC (ed) Modern methods for lipid analysis by liquid chromatography/mass spectrometry and related techniques. AOCS Press, Champaign, pp 61–178
31. Rezanka T, Siristova L, Melzoch K, Sigler K (2009) Direct ESI–MS analysis of O-acyl glycosylated cardiolipins from the thermophilic bacterium *Alicyclobacillus acidoterrestris*. Chem Phys Lipids 161(2):115–121
32. Rezanka T, Siristova L, Matoulkova D, Sigler K (2011) Hydrophilic interaction liquid chromatography: ESI–MS/MS of plasmalogen phospholipids from *Pectinatus* bacterium. Lipids 46(8):765–780
33. Bligh ED, Dyer WJ (1959) A rapid method of total lipid extraction and purification. Can J Biochem Biophysiol 37(8):911–917
34. Kates M (1986) Techniques of lipidology: isolation, analysis and identification of lipids. In: Work TS, Work E (eds) Laboratory techniques in biochemistry and molecular biology. Elsevier, Amsterdam, pp 220–223
35. Rezanka T, Dembitsky V (1999) Novel brominated lipidic compounds from lichens of Central Asia. Phytochemistry 51(8):963–968
36. Johnston NC, Goldfine H, Fischer W (1994) Novel polar lipid composition of *Clostridium innocuum* as the basis for an assessment of its taxonomic status. Microbiology 140(1):105–111
37. Rezanka T, Kambourova M, Derekova A, Kolouchova I, Sigler K (2012) LC/ESI–MS/MS identification of polar lipids of two thermophilic *Anoxybacillus* bacteria containing a unique lipid pattern. Lipids 47(7):729–739
38. Oulevey J, Bahl H, Thiele OW (1986) Novel alk-l-enyl ether lipids isolated from *Clostridium acetobutylicum*. Arch Microbiol 144(2):166–168
39. Hsu FF, Turk J (2006) Characterization of cardiolipin from *Escherichia coli* by electrospray ionization with multiple stage quadrupole ion-trap mass spectrometric analysis of $[M-2H + Na]^-$ ions. J Am Soc Mass Spectr 17(3):420–429
40. Mazzella N, Molinet J, Syakti AD, Barriol A, Dodi A, Bertrand JC, Doumenq P (2005) Effects of pure *n*-alkanes and crude oil on bacterial phospholipid classes and molecular species determined by electrospray ionization mass spectrometry. J Chromatogr B 822(1–2):40–53
41. de Vos P, Garrity G, Jones D, Krieg NR, Ludwig W, Rainey FA, Schleifer KH, Whitman WB (eds) (2009) Bergey's manual of systematic bacteriology, Volume three: The Firmicutes, Springer USA
42. Hsu FF, Turk J, Rhoades ER, Russell DG, Shi Y, Groisman EA (2005) Structural characterization of cardiolipin by tandem quadrupole and multiple-stage quadrupole ion-trap mass spectrometry with electrospray ionization. J Am Soc Mass Spectr 16(4):491–504
43. Hsu FF, Turk J (2006) Characterization of cardiolipin as the sodiated ions by positive-ion electrospray ionization with multiple stage quadrupole ion-trap mass spectrometry. J Am Soc Mass Spectr 17(8):1146–1157
44. Wayne LG, Brenner DJ, Colwell RR, Grimont PAD, Kandler O, Krichevsky MI, Moore WEC, Murray RGE, Stackebrandt E, Starr MP, Trüper HG (1987) Report of the Ad Hoc Committee on reconciliation of approaches to bacterial systematics. Int J Syst Bacteriol 37(4):463–464